Spatial Pattern Optimization for Intra-Cortical Stimulation with High-Density Multi-Electrode Arrays

Alessio Paolo Buccino, Tristan Stöber, Solveig Næss, Gert Cauwenberghs, Philipp Häfliger

Abstract—Recent advances in fabrication and processing techniques have made it possible to realize Multi-Electrode Arrays (MEA) with a very high density (HD). Such systems can not only be used to perform HD *in-vivo* recording, but they could also be used to actively stimulate neural tissue with high precision. While many studies have shown how HD MEA could help in identifying the neuron soma position and reconstruct the axonal arbor, here we aim at optimizing the stimulation capabilities of the MEA. We assumed that an estimate of the neuron position and axon hillock direction is available and we used a genetic algorithm to tailor the potential generated by the MEA in order to activate one or more target neurons by keeping the non-target or surrounding neurons at rest. We show that this approach allows to selectively excite neurons in a more robust and effective way with respect to conventional monopolar and bipolar stimulation.

I. Introduction

While there are many examples of successful very high density (HD) Multi-Electrode Arrays (MEA) developed for *in-vitro* recordings [1][2], the challenge of *in-vivo* recordings lies in the fact that there are much stricter size and power consumption limitations. New prototypes have been developed in the last years which attempt to overcome this limitation and to reach *in-vitro* high density also for *in-vivo* systems. The integration of HD MEA in CMOS technology can be achieved through the use of Electrolyte-Oxide-Semiconductor Field-Effect-Transistor (EOSFET), in which the gate of the transistor itself serves as sensor and it is coupled through a dielectric layer. In [3] a 16x16 matrix of electrodes with 15 µm pitch was fabricated on a single shank of 300 µm width and it was able to record HD Local Field Potentials. A great improvement is represented by the integration of recording and stimulation that could allow closed-loop experiments, with simultaneous recording and stimulation (as in [4]).
A system capable of both recording and stimulating neural tissue is very interesting especially for closed-loop experiments, in which stimulation is triggered from certain features extracted from recording the same neural sites. Such implants have the capability of inducing neuroplasticity *in-vivo* [5][6]. The main problem of recording-stimulation systems is the asymmetry between the two modalities. While for recordings it is relatively easy to reach a single-neuron discrimination by using spike sorting techniques, in stimulation tens or hundreds of µA are injected (or drawn) from electrodes and they spread radially in all directions. This results in a diffuse activation of neurons surrounding the stimulation site. [7] demonstrated that with spike-triggered stimulation not only the connection

between trigger and target neurons was strengthened, but also many non-target connections were affected and the entire neural network of recorded neurons changed its behavior. When studying neuroplasticity, it is definitely of great importance to be as selective as possible in order to be able to limit parasitic effect and to have a better controlled environment.

Recent studies have demonstrated that HD MEA allow to extract important information on the neuron's position and geometry. In [8], 144 neurons were localized (soma position) *in-vivo* with a 32 electrode MEA with 22-25 µm pitch. From another recent work [2] performed with HD MEA (17.5 µm pitch) *in-vitro*, not only neurons were localized, but axonal arbors were reconstructed using the redundancy of recordings and spike-triggered average. Certainly, *in-vivo* recordings are more noisy and less controllable, but it may be possible to exploit HD MEA to estimate the position of neurons surrounding the MEA and also to estimate the direction of propagation of the axon hillock.

In this work we assume that the previous information is available and we exploit the MEA to tailor stimulation spatial patterns to be as selective and as effective as possible with respect to the neuronal *scenario*. The goal is to show that spatial patterns can be optimized in order to depolarize specific target neurons, while not activating surrounding neurons. We show that it is possible to selectively activate target neurons and that the optimized spatial pattern outperforms the standard monopolar and bipolar stimulation in terms of robustness. The main limitation of this approach, though, is that in order to keep optimization fast and implementable online, simple models are used for the MEA stimulation, which introduce estimation errors, that should be quantified with more sophisticated models.

The article is organized as follows: Section II describes the methods involved in modeling, optimization, and simulation, Section III presents the results, and Section IV discusses the relevant findings and concludes the paper.

II. Methods

A. Modeling

The computational framework for performing the simulations was completely developed in Python, using custom models for the MEA and LFPy [9], based on Neuron [10], for the simulation of neural activation and responses.

The **MEA** was modeled as a NxN grid of monopolar current sources on a semi-infinite plane, with a pitch of 15 µm,

resembling the prototype described in [thewes]. The semi-infinite plane approximation is due to the fact that electrodes lie on a shank, facing the neural tissue only from one side. The potential at position $\vec{r}$ is

$$V(\vec{r}) = \sum_i \frac{I_i}{2\pi\sigma \left| \vec{r} - \vec{r_i} \right|}$$

where $\vec{r_i}$ and I_i are the position and current of the i-th electrode and σ is the conductivity of the tissue, assumed to be isotropic and homogeneous.

The **neurons** were modeled in a different way for evaluation and optimization. First, we used a simple neuronal model with a dendrite (L=100 μm, D = 1 μm), a soma (L=19 μm, D = 19 μm), a cone-shaped axon hillock (L=10 μm, D = from 19 to 1 μm), and an axon tract (L=90 μm, D = 1 μm). When the neuron is modeled with the cable equation, the effective de/hyperpolarization can be predicted with the so called acivation function (AF) [11], which is the second order derivative of the external potential along the neuron's direction scaled by the squared of the space constant ($AF = \lambda^2 \frac{\partial^2 V_e}{\partial x^2}$). A test neurons was placed at 15 μm from a monopolar electrode coincident with the center of the soma, or two bipolar electrodes, with the cathode (negative current) coincident with the soma and the anode (positive) in the axon direction. Different current intensities were then applied with a monophasic 100 μs pulse and the minimum AF (for the rest of the paper we will refer to AF as the second derivative only, withouth the λ^2 scaling) required to generate a spike was *empirically* evaluated and served as activation threshold for the optimization step.

For optimization of the spatial pattern a neuron is represented by a single segment starting from the soma location, with the direction of the axon hillock. Hence, a *geometric neuron* consists of a 3D point (soma), an alignment (axon hillock direction), and a length (which was set to 15 μm). The optimization searches for solutions (current values on the different electrodes) that excite the target neuron and keeps the surrounding neurons at rest.

B. Optimization

The optimization framework is implemented using DEAP package [12]. Genetic algorithms perform optimization with a stochastic approach, by randomly sampling the solution space (in this case the currents to be assigned to each electrode) and evaluating them with a fitness function. This approach has been selected for its speed and customizability. The fitness function plays a very important role and is the key to achieve a good optimization. Let us summarize the objectives of stimulation: the first objective is depolarizing the target neuron by applying an AF above threshold with a safety margin. At the same time we want to find a spatial pattern that does not generate spikes on non-target neurons. Second, we encourage sparse and energy efficient solutions, since they would be easier to implement and consume less power. This said, the fitness function is in the form of:

$$\begin{cases} f_1 = \alpha x_{target} + (1-\alpha)x_{surround} \\ f_2 = \beta x_{sparsity} + (1-\beta)x_{energy} \end{cases} \quad (1)$$

where x_{target} is a hinge loss-like function that penalizes if the maximum AF point along the target neuron is below the activation threshold; $x_{surround}$ penalizes all points of non-target neurons whose AF is above the non-activation threshold, $x_{sparsity}$ and x_{energy} represent the normalized (between 0 and 1) sparsity of the solution (zero-current electrodes/total electrodes) and energy efficiency (sum of absolute currents/maximum deliverable currrent). The 2 objectives (f_1 and f_2) are maximized with the same weight, so that the solution will then represent a trade-off among these two objectives. The parameters α and β can be adjusted to favor target activation versus non-target inactivation and sparsity versus energy efficiency. In order to keep in mind a possible physical implementation of the system, some constraints on the value of currents have been added. In particular the currents can go from -20 μA to +20 μA , but they can only have 2 μA steps. Therefore, currents can have 21 different values, but a negative current is the opposite of the positive one, so only 10 values (excluding 0) can be generated.

Selection of the solutions to be mated was performed with a selection tournament approach. Two-point crossover operator has been used and applied with 80% probability. Mutation was applied to 10% of the population and it consisted of 2 steps: in the first step a gaussian mutation was applied with 20% probability to each current value; then, in order to favor sparse solution 20% of the current values were randomly set to 0 to favor energy efficient solutions. The best solutions of each iteration were always kept in the offspring. The genetic algorithm was run for 300 generations and it was stopped after 100 generations of stall.

C. Simulation

In order to compare the performance of the optimized spatial pattern with respect to conventional monopolar and bipolar approaches, 1000 *scenarios* were simulated and different figures of merit were computed. In the proximity of a 4x4 MEA (in the *y-z* plane, centered at (0, 0, 0)) one target neuron was randomly placed between 5 and 15 μm from the MEA (in the *x* direction), while 4 surrounding neuron were placed randomly between 5 and 30 μm, with the constraint of the somas of adjacent neurons being more distant than 15 μm. The alignment of the axon hillock was random in the *y* and *z* direction and it was 0 in the *x* direction (neurons are assumed to be parallel to the MEA plane). Three different stimulation approaches were compared: the genetetic algorithm (GA) optimized spatial pattern, the monopolar stimulation (MONO), in which the closest electrode to the mid point of the neuron was set to -10 μA, and the bipolar stimulation (BI), in which the closest electrode to the end point of the neuron was set to +10 μA and added to the monopolar electrode.

The GA optimization for each scenario was run as described in Section II-B using an activation threshold of 1.5 mV^2/μm^2, a non activation threshold of 0.5 mV^2/μm^2, an α of 0.4 and a β of 0.5. The activation threshold was chosen based on the empirical evaluation described in Section II-A, which showed that a second derivative of the potential along the neuron of
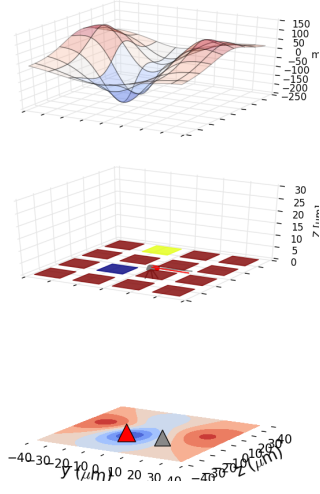
Figure 1. *Top:* Target neuron (red) and surrounding neurons (grey) with MEA. Colors are current amplitudes. *Middle:* Potential surface at $x = 15$ μm. *Bottom:* 2D projection of potential, MEA, and neurons.

1.5 mV^2/μm^2 consistently generates spikes in both monopolar and bipolar configurations.

III. RESULTS

A. Sample Scenario

First, let us analyze one of the random *scenarios*. The top panel of Fig. 1 shows the 3D position and direction of the neurons, as well as the MEA electrode locations. The larger cylinders represent the somas, while the narrower ones are the axon hillock direction. It can be noticed how the configuration can be intricated and tangled, depending on the relative alignment between the target and surrounding neurons and their relative distance. The colors on the MEA depicts the intentsies of the applied currents. In the central panel the potential generated by the MEA on the plane $(15$ μm, x, $y)$ is displayed as a 3D surface. It can be appreciated how troughs and hills are shaped so that the target neuron falls in a positive AF region, while the surrounding neurons do not. The bottom panel shows a contour plot of the field and the projection of the neurons on the MEA plane $(0, x, y)$ and the 2D projection o the neurons on the same plane.

Fig. 2 shows the trends of the AF for the target neuron (red) and surrounding neurons (grey). It is clear that the optimized
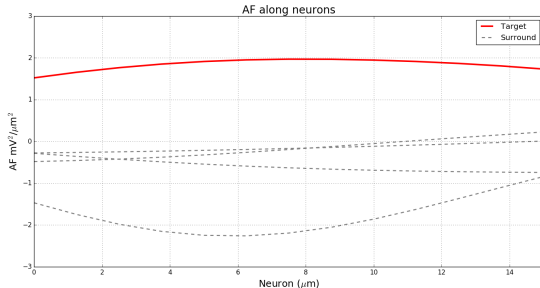

Figure 2. AF trend along the neuron for the target neuron (red) and the surrounding neurons (gray)

Target	mean	median	max	min	sd	%max>threshold
GA	2.09	1.68	16.9	1.5	1.29	**100%**
MONO	2.154	1.40	16.3	-4.74	3.01	48%
BI	1.83	1.29	18.14	-16.1	4.04	45.6%

Table I
PERFORMANCE ON TARGET NEURON. MEAN, MEDIAN, MAX, MIN, AND SD ARE THE AVERAGE OVER THE 1000 *scenarios* OF THE AF ALONG THE TARGET NEURON

spatial pattern, for this *scenario*, is able to pull the AF above the activation threshold almost for all the points of the target neuron and to keep the non-target neurons' AF below the threshold with a relatively large margin. However, it should be noticed that there is a lot of variability among *scenarios* and not always the GA achieves the objectives. Nevertheless, even if the threshold is not reached, the target neuron's AF is pulled as high as possible as long as the surrounding neurons are kept at rest.

B. Genetic Algorithm, Monopolar, and Bipolar Comparison

The performance of stimulation concerns both the activation of the target neuron and the non-activation of the non-target neurons. In each scenario, the AF is computed on 15 points (every 1 μm), hence for every *scenario* different metrics are computed from the AF of each neuron. In Table I the average of each of these values among the entire 1000 *scenarios* for the target neuron is shown. The mean and median values are greater for GA than for MONO and BI, while the maximum is less, implying that the AF trend is more constant for GA. Moreover, the last column shows the percent of *scenarios* in which the maximum AF value is above threshold, i.e. the target is activated. The GA pattern is able to stimulate the neuron in 100 % of the cases, more reliably than the monopolar (48 %) and bipolar (45.6 %).

In order to evaluate the selectivity of the stimulation we considered the surrounding neuron with the highest AF. If a non-target neuron's AF gets close to the activation threshold, then it is likely that a spurious spike is generated. In Table II the statistics of the maximum values among the non-target neurons are displayed. The values are overall smaller for the GA approach, especially the maximum value of the AF. From the last column, which shows the percentage of surrounding neurons (in this case all the surrounding neurons are considered, not only the one with highest AF) whose AF reaches the activation threshold of 1.5 mV^2/μm^2, it can be appreciated how the GA is more robust than MONO and BI, since it pulls non-target neurons above threshold only in 0.8 % of the cases, compared to the 16.7 % of the monopolar approach and the 22.3 % of the bipolar one.

Fig. 3 displays the boxplots of the distributions of the maximum surround AF (the same values shown in II), divided between the 3 approaches (GA, MONO, BI). The higher selectivity and robustness of the GA stimulation is reflected in the less number of outliers, which means that in less cases spurious spikes are generated. Moreover, the values of the AF above the activation threshold (1.5 mV^2/μm^2, blue horizontal line) are higher for MONO and BI approach, due to their lower
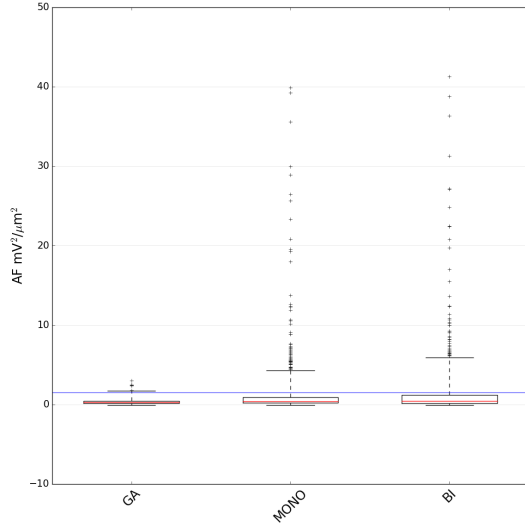
Figure 3. Boxplots of maximum AF on surrounding neurons divided by stimulation approach (GA, MONO, BI). The blue horizontal line is the activation threshold of 1.5 mV^2/μm^2

adaptation to the environment, especially to the surrounding neurons' position.

It is interesting to analyze to output of the GA also in terms of sparsity and energy efficiency. In 50.3% of the cases the GA outputs a monopolar pattern, but it should be emphasized that the intensity of the current is adapted to the scenario. In 87% of the cases, instead, only 3 or less electrodes are involved in the spatial pattern. The *convergence* of the GA to a monopolar- or bipolar-like solution when the *scenario* is not too complex is ensured by the sparsity and energy efficiency terms in the fitness function (Eq. 1), which tries to maximize the number of non-active electrode and the current delivered from each electrode. On average, among all 1000 *scenarios*, the total amount of delivered current is 21.26 μA, almost the same as the bipolar approach (which delivers 20 μA).

IV. DISCUSSIONS AND CONCLUSION

In this study we presented a novel approach to exploit the high density of MEA for improving stimulation selectivity and adaptation. We showed that the proposed method is more selective and robust than standard monopolar and bipolar approaches, even if it would require more energy consumption and a more complex control.

In order to speed up the optimization and possibly make it implementable also in an online setup, we used monopolar current source approximation a simple model for the MEA.

Non-Target	mean	median	max	min	sd	%max>threshold
GA	0.15	0.15	0.3	0.05	0.37	**0.8%**
MONO	0.46	0.46	1.27	0.11	0.51	16.7%
BI	0.45	0.45	1.45	0.08	0.95	22.3%

Table II
PERFORMANCE ON NON-TARGET NEURONS. THE VALUES REFER TO THE SURROUNDING NEURONS WITH THE HIGHEST VALUE FOR THE DIFFERENT METRICS.

Clearly, the geometry of the electrodes play an important role; hence, the error between the monopolar current source approximation and a more accurate method, such as a Finite Element Methods (which has been applied to MEA in [13]), should be characterized for an *a-posteriori* evaluation.

Moreover, we assumed to be able to estimate the exact position of the neurons' somas and to be able their axon hillock direction from recorded data. This is definitely a strong assumption, but previous studies showed that HD MEA are capable of providing such information [8][2]. Nevertheless, the estimation error involved in this step should be evaluated as well, and our future work will deal with the entire loop: from recorded data, to position and direction estimation, to stimulation and evaluation of the outcome on more complex neural models, as well as *in-vivo*.

In conlusion, we introduced an optimization approach for neural stimulation with HD MEA, which could lead to the capability of robustly targeting single neurons with extra-cellular electrical stimulation.

V. ACKNOWLEDGMENTS

REFERENCES

[1] L. Berdondini, A. Bosca, T. Nieus, and A. Maccione, "Active pixel sensor multielectrode array for high spatiotemporal resolution," in *Nanotechnology and Neuroscience: Nano-electronic, Photonic and Mechanical Neuronal Interfacing*. Springer, 2014, pp. 207–238.

[2] J. Müller, M. Ballini, P. Livi, Y. Chen, M. Radivojevic, A. Shadmani, V. Viswam, I. L. Jones, M. Fiscella, R. Diggelmann *et al.*, "High-resolution cmos mea platform to study neurons at subcellular, cellular, and network levels," *Lab on a Chip*, vol. 15, no. 13, pp. 2767–2780, 2015.

[3] S. Schroder, C. Cecchetto, S. Keil, M. Mahmud, E. Brose, O. Dogan, G. Bertotti, D. Wolanski, B. Tillack, J. Schneidewind *et al.*, "Cmos-compatible purely capacitive interfaces for high-density in-vivo recording from neural tissue," in *Biomedical Circuits and Systems Conference (BioCAS), 2015 IEEE*. IEEE, 2015, pp. 1–4.

[4] S. Ha, C. Kim, J. Park, S. Joshi, and G. Cauwenberghs, "Energy-recycling integrated 6.78-mbps data 6.3-mw power telemetry over a single 13.56-mhz inductive link," in *VLSI Circuits Digest of Technical Papers, 2014 Symposium on*. IEEE, 2014, pp. 1–2.

[5] A. Jackson, J. Mavoori, and E. E. Fetz, "Long-term motor cortex plasticity induced by an electronic neural implant," *Nature*, vol. 444, no. 7115, pp. 56–60, 2006.

[6] D. J. Guggenmos, M. Azin, S. Barbay, J. D. Mahnken, C. Dunham, P. Mohseni, and R. J. Nudo, "Restoration of function after brain damage using a neural prosthesis," *Proceedings of the National Academy of Sciences*, vol. 110, no. 52, pp. 21 177–21 182, 2013.

[7] J. M. Rebesco, I. H. Stevenson, K. Koerding, S. A. Solla, and L. E. Miller, "Rewiring neural interactions by micro-stimulation," *Frontiers in systems neuroscience*, vol. 4, p. 39, 2010.

[8] I. D. Ruz and S. R. Schultz, "Localising and classifying neurons from high density mea recordings," *Journal of neuroscience methods*, vol. 233, pp. 115–128, 2014.

[9] G. T. Einevoll, "Lfpy: a tool for biophysical simulation of extracellular potentials generated by detailed model neurons," 2014.

[10] N. T. Carnevale and M. L. Hines, *The NEURON book*. Cambridge University Press, 2006.

[11] F. Rattay, *Electrical nerve stimulation*. Springer, 1990.

[12] F.-A. Fortin, D. Rainville, M.-A. G. Gardner, M. Parizeau, C. Gagné *et al.*, "Deap: Evolutionary algorithms made easy," *The Journal of Machine Learning Research*, vol. 13, no. 1, pp. 2171–2175, 2012.

[13] S. Joucla, A. Glière, and B. Yvert, "Current approaches to model extra-cellular electrical neural microstimulation." *Frontiers in computational neuroscience*, vol. 8, pp. 13–13, 2013.